PREDICTION OF SPECTRAL SHIFTS PROPORTIONAL TO SOURCE DISTANCES BY TIME-VARYING FREQUENCY OR
WAVELENGTH SELECTION

V. Guruprasad

Inspired Research, New York, USA.

Optical Engineering
+Applications
Part of SPIE Optics+Photonics
Nature of Light: Light in Nature II – 11 Aug 2008

inspired research

ABSTRACT

Drift in front-end frequency or wavelength selection should cause observed spectra to be variously and simultaneously scaled *in proportion to their source distances.* The reason is that detectors after the drifting selection would integrate instantaneous electric or magnetic field values from successive sinusoids in the received spectrum differing in both frequency and phase. Phase differences between frequencies are ordinarily irrelevant, and current recalibration procedures at most correct frequency errors.

With a drifting selection, each instantaneous field value is obtained from the sinusoid possessing the instantaneously selected frequency *at its instantaneous received phase.* The detector integration will therefore construct waveforms that follow the drifting selection but with acceleration of phase equal to the rate of the drift times the slope of the received phase spectrum. Phase acceleration in itself constitutes frequency shifts. These shifts would be additionally proportional to source distances because the path delay presents phase offsets proportional to the frequency times the distance, eventually exceeding initial phase differences and making the slope of the phase spectrum an asymptotic measure of the source distance.

Tuneable optics is expected to soon become fast enough for realizing such shifts by Fourier switching. Envisaged applications include pocket X-ray devices; wave sources continuously variable from RF to gamma rays; capacity multiplication with jamming and noise immunity in fibre and radio channels; elimination of the need for frequency allocations; accurate passive ranging and navigation from ground to deep space; and so on.

1. PREMISES AND DERIVATION

Detector response, both classically and in quantum mechanics, is characterized by the Hilbert dot product of detector eigenfunctions $\langle\psi| \equiv \psi^*(t)$ with the received wavefunctions $|f\rangle \equiv f(t)$, defined by $\langle\phi|f\rangle = \int \phi^*(t)\, f(t)\, dt$. For ordinary Fourier spectral analysis, the domain of integration is in theory from $t = -\infty$ to $+\infty$, and in Fourier spectrometry, the eigenfunctions $\langle\phi|$ are sinusoids or, equivalently, the purely imaginary functions of the form $e^{i\omega t}$, where ω signifies the angular frequency. The corresponding dot products are then of the form

$$\langle\psi(\omega)|f\rangle \equiv \langle\omega|f\rangle = \int e^{-i\omega t}\, f(t)\, dt \equiv F(\omega) \quad , \tag{1}$$

where the rightmost term $F(\omega)$ is the common notation for the Fourier transform for the time-domain function $f(t)$, given by the inverse transform

$$\langle t|f\rangle \equiv \int |\omega\rangle\, d\omega \langle\omega|f\rangle \equiv \int e^{i\omega t}\, F(\omega)\, d\omega \equiv f(t) \quad . \tag{2}$$

In quantum mechanics, the eigenfunctions $\psi^*(t)$ represent detector states and the dot products $\langle\psi|f\rangle$ represent probability amplitudes. In classical electromagnetics theory, the function $f(t)$ invariably refers to the electric or magnetic field intensity arriving at the detector, and the square of the dot product represents the actual power density at that (angular) frequency. The present treatment is classical, but as the equations remain identical in form, the results should hold also in the quantum picture.

The key issue treated here for the first time is the physical separation that exists between frequency or wavelength selection mechanisms, such as diffraction gratings and prisms in optics or the sampling interval in digital signal processing (DSP), and actual measurement of the Fourier amplitudes $F(\omega)$ by photodetectors, which invariably occurs *after* the selection in spectrometry.

A photodetector can only integrate whatever sequence of electric (or magnetic) field values that arrive at its input, regardless of whether those are the actual values emitted by the source, or became manipulated *en route*. The specific manipulation considered is *time-varying, or chirped, frequency or wavelength selection,* quantified by the *normalized rate of change* of the wavevector k, the (angular) frequency ω or the wavelength λ, respectively, as

$$\beta \equiv k'^{-1}\,dk'/dt \equiv \omega'^{-1}\,d\omega'/dt \equiv -\lambda'^{-1}\,d\lambda'/dt, \tag{3}$$

where the primes denote the instantaneous selection. Such a time-variation would result from a uniform variation of the intervals in a diffraction grating, or from variation of the refractive index of a prism, or of sampling intervals in DSP. In all cases, the detector's integration would be transformed into

$$
\begin{aligned}
\langle \omega'', \beta | f, r \rangle &\equiv \int_t \langle \omega'', \beta | t \rangle\, dt \int_\omega \langle t | \omega \rangle\, d\omega\, \langle \omega | f, r \rangle \\
&= \int_\omega \int_t e^{-i\omega'' t}\, dt \left[e^{i(d\phi''/dt)(t-r/c)} F(\omega)\, d\omega \right] \qquad \text{(inverting the order of integration)} \\
&= \int_\omega e^{-ik'' r} \delta(\omega'' - \omega\Delta) F(\omega)\, d\omega = e^{-ik'' r} F(\omega''/\Delta) \qquad (k'' \equiv \omega''/c) \quad ,
\end{aligned}
\tag{4}
$$

where the double primes generally refer to values arriving at the detector, and

- the notation $|f, r\rangle$ gives cognizance to the path delay r/c from the source;
- the detector eigenfunctions $\langle \omega'', \beta |$ refer to the (angular) frequency ω'' actually seen by the detector and the changing selection represented by the rate β;
- $\Delta \equiv (1 - v/c + \beta r/c)$, $v \equiv \dot{r} \equiv dr/dt$ denoting relative motion of the source, as will be derived below;
- and in the second step, we have written $d\phi''/dt$, the instantaneous rate of change of phase of the waveform comprising the sequence of field values arriving at the detector, for ω'', to explicitly represent the variation of selection over time.

The scale factor Δ is obtained from a careful accounting of all of the phase contributions occurring between the source and the detector, including an initial phase offset $-\phi^s$ at the source; path delay from the source to the grating $-\omega r/c$; an additional phase change $-\phi^g$ due to transmission by the grating; and the path delay $-\omega\rho/c$ from the grating to the detector, where ρ is the grating-detector path (Fig. 1), so that

$$\phi'' = \omega t - \phi^s - \omega r/c - \phi^g - \omega\rho/c \quad . \tag{5}$$
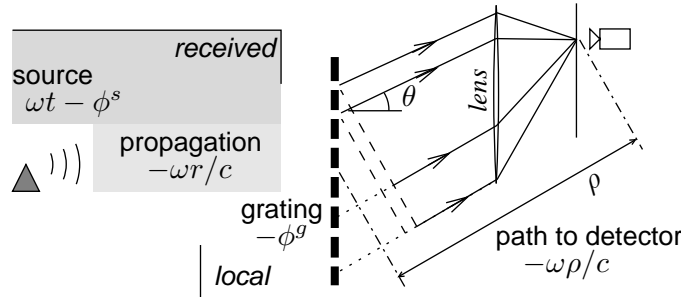
Fig. 1. Phase contributions in Fourier spectrometry

Since frequency or wavelength selection cannot affect path delays or source phase offsets, we should find that

$$\frac{d\phi''}{dt} = \left[\frac{d\phi}{dt} - \frac{d\phi^s}{dt} - \frac{d(\omega r/c)}{dt} \right] - \left[\frac{d\phi^g}{dt} + \frac{d(\omega\rho/c)}{dt} \right] \quad . \tag{6}$$

The first term on the right, $d\phi/dt$, itself comprises the intrinsic rate of change of phase represented by the original angular frequency ω, and an additional part due to the changing wavelength selection, as

$$\frac{d\phi}{dt} = \frac{\partial\phi}{\partial t} + \frac{\partial\phi}{\partial k'} \frac{dk'}{dt} \equiv \omega + \dot{k}' \frac{\partial\phi}{\partial k'} = \omega \quad . \tag{7}$$

The second term on the right in equation (6) expands similarly, except that $\partial\phi^s/\partial t \equiv 0$ as ϕ^s are constants with respect to time, but $\dot{k}'\,\partial\phi^s/\partial k'$ survives because ϕ^s would likely vary across wavelengths, and hence across successive values of k'. For constant wave speed c, the remaining terms similarly expand to

$$\frac{d(\omega r/c)}{dt} = \dot{r}\,\frac{\partial(kr)}{\partial r} + \dot{k}'\,\frac{\partial(kr)}{\partial k'} = k\dot{r} + \dot{k}'r, \quad \frac{d\phi^g}{dt} = \frac{\partial\phi^g}{\partial t} + \dot{k}'\,\frac{\partial\phi^g}{\partial k'} \quad , \text{ and } \quad \frac{d(\omega\rho/c)}{dt} = \dot{k}'\,\frac{\partial(k\rho)}{\partial k'} = \dot{k}'\rho \quad , \tag{8}$$

noting that $k \equiv \omega/c$ generally, and $\dot{\rho} = 0$ for a static focusing lens assembly. If the selector is a diffraction grating, $\partial\phi^g/\partial t$ cannot vanish while the grating intervals are varied, but we could move the photodetector keeping the grating fixed to get the same variation of selection, for which $\partial\phi^g/\partial t = 0$. In either case, equation (6) leads to

$$d\phi''/dt \equiv \omega'' = \omega - k\dot{r} - \dot{k}'(r + \rho + \phi^s_{,k'} + \phi^g_{,k'}) \quad (_{,k'} \equiv \partial/\partial k') \quad . \tag{9}$$

Absorbing ρ into r, replacing $\dot{r}$ with v, and noting that $k' \equiv k$ because the output and input wave vectors at the grating would be identical at each instant, we get

$$
\begin{aligned}
\omega'' \equiv \dot{\phi}'' =\ & \omega(1 - v/c + [r + (\phi^s_{,k} + \phi^g_{,k})]\beta/c) \\
\simeq\ & \omega(1 - v/c + \beta r/c) \quad, \\
\text{and } z(r) \equiv \delta\omega/\omega \equiv\ & (\omega'' - \omega)/\omega = -v/c + [r + (\phi^s_{,k} + \phi^g_{,k})]\beta/c \\
\simeq\ & -v/c + \beta r/c \quad,
\end{aligned}
\tag{10}
$$

yielding the Δ of equation (4). $\square$

2. SOURCE DISTANCE INFORMATION IN PHASE

Absolute distance information is not ordinarily expected to be present in wave phase principally because of the common misconception of waves as inherently periodic, if not more specifically sinusoidal. Physicists invariably forget that sinusoidal waves are merely the eigenfunctions of the Fourier decomposition of arbitrary waveforms, the general solution of the basic wave equation $(\nabla^2 + \mathbf{k}^2)\psi = 0$ being merely a linear combination of all possible travelling functions $f(\mathbf{k}\cdot\mathbf{r} \pm \omega t)$, with *no constraint on the shape of f*. The periodicity intuition comes from the related observation that discrete combinations of sinusoids are periodic, as known from Fourier series theory.

The common notion that the phase of a wave cannot reveal the absolute distance to its source comes partly from interferometry and holography, including synthetic aperture radar imaging, which involve interference between sinusoids of the same frequencies. The interference patterns invariably display periodicity. In pulse radar imaging, multiple wavelengths of interrogation are available due to the frequency comb generated by the pulse train, and reveal the target features along the radial direction, but the absolute range to the target must still be estimated from the total round trip time of the echos. This usual perception is incorrect for two reasons:

- Since the transport of energy or information implies finite beginning and end, a travelling waveform spectrum cannot be discrete and must be inherently continuous, requiring a Fourier transform, and not merely a Fourier series decomposition, to permit exact inversion. This is stated as Lemma 2.1 in the paper.

  The proof provides relevant insight. We may impose a finite compact support $[0, T]$ on an arbitrary waveform $g(x)$, by multiplying $g(x)$ by

  $$u_{[0,T]}(x) \triangleq \begin{cases} 1 & \text{for } x \in [0, T] \\ 0 & \text{otherwise} \end{cases} \tag{11}$$

  and use the product $g(x).u_{[0,T]}(x)$ to describe a travelling waveform. Its spectrum would be the convolution product $G(\nu) \circ U_{[0,T]}(\nu)$, where $G(\nu)$ is the Fourier transform of $g(x)$, and $U_{[0,T]}(\nu)$ is the Fourier transform of $u_{[0,T]}(x)$, given by $U_{[0,T]}(\nu) \equiv 2T^{-1}e^{iT\nu/2}\,\text{sinc}(2\nu/T)$, where $\text{sinc}(\xi) \equiv \sin(\xi)/\xi$ is continuous and infinite. Even if $G(\nu)$ itself were discontinuous, say a set of impulses, $U(\nu)$ would make the convolution product $G \circ U$ continuous and infinite, as shown for a pulse train over time in Fig. 2.
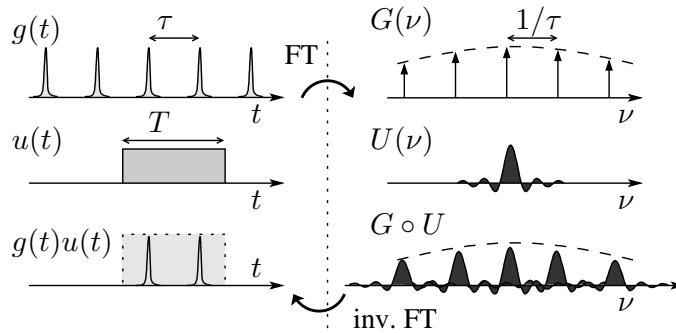

Fig. 2. Spectral continuity

At optical wavelengths, the Doppler linespreads due to thermal motions at the source and the detector jitter due to noise ordinarily mask this property. However, all of radio communication technology today depends on

the ability of receivers to tune into signals that are otherwise too weak to induce observable currents. The fact that this continuum of spectral components would be consistent in phase, and thus mutually coherent, is of particular significance, as will become clear in Section 3.

- A truly continuous spectrum means that, at least in principle, it should be possible to select infinitesimally close pairs of frequencies. As the frequency of the "beat wave" between such a pair tends to 0, its wavelength tends to ∞, so that its phase never repeats. That is, *differential beat waves are aperiodic and do carry absolute source distance information* as a result, proved as Lemma 3.1 in the paper.

  The approach requires normalized wavelength resolutions of 10^{-11}, i.e., this fraction of a fringe in terms of interferometry, to resolve distances up to 10 km. It is thus impractical, but invalidates the usual preception.

A more practical solution is related to the method of Green's functions for solving integro-differential equations. Green's functions are trial functions corresponding to point impulse sources, of the form $\psi = s^{-1}e^{iks}$, where s denotes distance from the point source to the point of integration (see [1, Chapter 8.3]). The generality of this approach stems from the basic equivalence of an arbitrary source to a space-time distribution of point impulses, so that electromagnetic potential distribution and wave propagation both become integrals of Green's function solutions over all such source distributions. An inseparable property of these Green's functions, which hitherto had little significance of its own, is that *all of the component sinusoids would have the same initial phase of zero*, because the phase factor e^{iks} in the Green's functions does not include a phase offset! This is illustrated in Fig. 3 below, which shows how the sinusoidal components must then evolve in phase with distance r from the source.
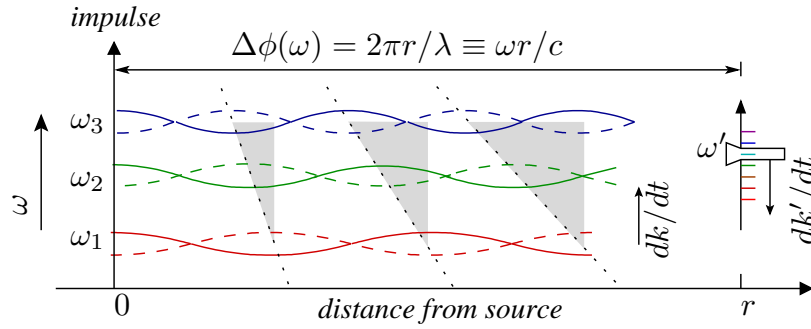

Fig. 3. An implication of Green's theorem

The Green's function perspective leads to an even broader result, viz *that at distances beyond a few wavelengths, the phase differences between the tonal components of most waveforms emitted by a finite source become linear measures of source distance.* The reason is that as Fig. 3 shows, the phase of each tone increases linearly with the distance r from its source, and at a rate proportional to its own frequency, so that the differences can be used to compute r. It was assumed for the figure that the tones started with the same phase at the source, which is only valid for a Green's function. However, the initial phase values of the components of even an arbitrary waveform can only differ by $\pm\pi$, hence the result.

Phases and phase differences are harder to measure than frequencies. The shaded triangles in Fig. 3 show further that *at large distances, the slope of the phase spectrum is a direct measure of the distance to the wave origin*, i.e.

$$\frac{\partial\phi/\partial k}{r} = 1 + \frac{\partial \log F/\partial k}{ir} \longrightarrow 1 \quad \text{as} \quad r \longrightarrow \infty \quad , \tag{12}$$

as proved in Lemma 3.2 in the paper, where F is the ordinary Fourier spectrum of the waveform. Our time-varying selection multiplies into this slope to yield the main frequency shift term $\dot{k}'\partial\phi/\partial k'$, in equation (7).

3. PRINCIPLES OF CHIRPED DECOMPOSITION

The only difference in equation (4) from the traditional Fourier analysis is the temporal variation of the (angular) frequency selection ω', which, although not present in equation (4), calls for re-evaluation of the rate of change of phase arriving at the detector, and hence of the detected frequencies. With changing selection, the instantaneous (angular) frequency ω'' of the waveform seen by the detector would be following the changing selection ω', and cannot be any one of the original component pure tones that arrived at the selector front-end even for a fraction of a cycle. Specifically, we would expect the following:

A. The time-varying selection and subsequent detection should exhibit eigenfunctions of time-varying frequency, i.e., chirps, given by

$$\langle\omega'| \equiv e^{-i\omega'(t)\,t} \quad , \text{ where } \omega'(t) = \omega'(0)\,e^{\beta t} \quad , \tag{13}$$

consistent with equation (3). The chirps form a two-dimensional Hilbert basis of their own, since

$$\langle \omega'_p | \omega'_q \rangle \equiv \int e^{-i\omega'_p(t)\,t}\, e^{i\omega'_q(t)\,t}\, dt \propto \delta_{\omega'_p, \omega'_q} \equiv \delta_{\beta_p, \beta_q} . \delta_{\omega'_p(0), \omega'_q(0)} \quad , \tag{14}$$

so that the rates of change and the frequencies at some instant must both agree for a nonvanishing product.

B. The chirps would be orthogonal to the original pure tone components, i.e.,

$$\langle \omega' | \omega \rangle \equiv \int e^{-i\omega'(t)\,t}\, e^{i\omega t}\, dt \simeq 0 \quad . \tag{15}$$

However, the result is exact only for integration over infinite time. Practical integrations would be over finite intervals with finite sample resolutions, resulting in small values corresponding to at most a few samples in the discrete Fourier transform sum corresponding to the integration. What this means is that a continuous-wave (CW) monochromatic source will vanish from the detected waveform. *To be detected by chirp decomposition, a source waveform must possess a continuous nonzero interval of tones, or equivalently, have discontinuities in the time domain, which would represent information transport.* This and the next property are graphically explained with an example in Fig. 3, comprising a chirp $y = \sin(x^{1.8}/30)$, approximating an exponential chirp, and two pure tones $y_1 = \sin(2\pi x/3.2 - 0.55)$ and $y_2 = \sin(2\pi x/2.5 + 0.60)$, respectively. As the graph illustrates, each pure tone coincides with the chirp for at most a fraction of a cycle, as marked by the arrows.
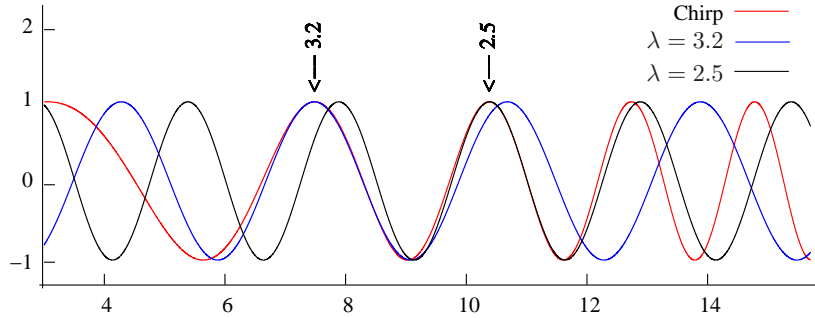

Fig. 3. Tonal components of a chirp

C. The fractional cycle coincidence with a pure tone occurs at *a distance proportional to the tonal frequency* in reverse direction to increasing chirp frequency. Thus, in Fig. 3, the chirp coincides with the higher frequency (3.2) tone to the left of its coincidence with the lower frequency (2.5) tone, and the chirp wavelength decreases towards the right. The proportionality to distance reflects the frequency variation of the chirp. In particular, *if the original waveform f contained a succession of pure tones at just the right phases at their respective frequency coincidences, the "chirp amplitude" $\langle \omega' | f \rangle \equiv \int e^{-i\omega'(t)\,t}\, f(t)\, dt$ would be substantial.*

Equation (12) says that this condition of matching phases at distances proportional to the frequencies is asymptotically satisfied by the ordinary Fourier components of any waveform emitted by any wave source.

D. Corresponding to the orthogonality condition (14), the fractional cycle coincidences contributing to the chirp amplitude $\langle \omega' | f \rangle$ must themselves depend on the initial value $\omega'(0)$ as well as the rate of change β.

For different values of $\omega'(0)$, the exponential chirp amplitude $\langle \omega'_0, \beta | f \rangle \equiv \int \exp(-i\omega'_0\, e^{\beta t}\, t)\, f(t)\, dt$ will vary vastly, as the component tones of f would have fractional cycle coincidences only around some initial values ω'_0 for any given β, and conversely, around some β for a given ω'_0.

Chirp spectra are thus characterized by the two parameters β and ω'_0. They replace the frequency ω and phase ϕ characterizing Fourier spectra, but are otherwise distinct and call for an independent interpretation. For the same starting frequency ω'_0, different normalized shifts $z(r)$ will result at different values of β for the same source distance r, and conversely, different z will result for the same β for sources at different distances r, r', etc., as illustrated in Fig. 5. This permits an interpretation of β as a *temporal form of parallax*, in which the receiver can move with respect to the temporal frequencies of a source, just like it moves relative to the spatial frequencies, to reuse a notion from Fourier holography, in ordinary (spatial) parallax.
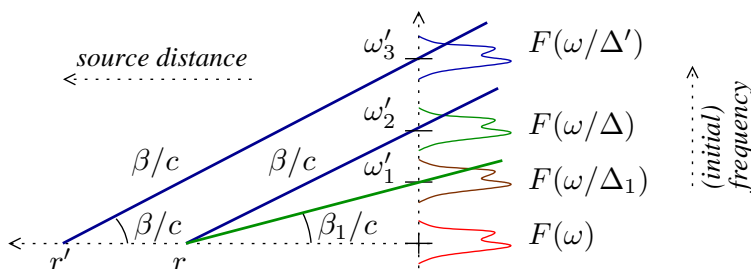
Fig. 5. Chirp offset and rate spectra

Also, with any given source and using a fixed β, we should get substantial chirp amplitudes at different ω_0' from the fractional cycle coincidences of different sets of frequencies from the source. Higher initial frequencies ω_0' means higher source frequencies contribute to the chirp amplitude, hence ω_0' *corresponds to the frequency axis of the Fourier spectrum*. In fact, the same variation of grating intervals, or of the sampling interval in a DSP system, would cause all of the receiver eigenfunctions, corresponding to different selections ω', to vary simultaneously at the same normalized rate (β). Hence the applied variation can be regarded as transforming Fourier spectra into chirp spectra, by the mapping $\omega' \to \omega_0'$, corresponding to motion of the instrument scale in Fig. 3.

4. BROADER IMPLICATIONS

Rigorous test of spectral continuity

In solid state physics, the electron conduction band is really *quasi-continuous*, as the Bloch states are stationary states and are therefore inherently discrete, albeit very close together. In scattering and photoelectricity theories, incident radiation is considered to have an inherently continuous energy spectrum, which leads to interaction matrices of mixed cardinality linking the continuum of radiation states with the inherently discrete bound states in matter. However, the resulting interaction literally relates the discrete bound states to a corresponding discrete subset of the radiation continuum! Continuous spectra are involved in the Compton scattering and the Doppler effect, but observations of the affected light are inherently constrained by the quantized nature of photodetection! Even with Mössbauer spectroscopy, we would be limited to testing spectral continuity one frequency at a time, and therefore still unable to fundamentally distinguish between continuous and quasi-continuous spectra.

The present effect provides the first direct dependence on spectral continuity, similar to a velocity or a momentum in the time domain. More precisely, it extracts coherence across frequencies, whereas all prior notions and tests of coherence hitherto concerned phase correlation only within the same frequency (cf. [1, Chapter X]).

Reconstitutability of photons

Application of Planck's quantization rule $E = h\nu \equiv \hbar\omega$, originally defined in the context of standing wave modes, more generally to radiation in photoelectricity and scattering theories requires assuming either that radiation is only observed in discrete quantities at each frequency, or that it is inherently quantized even in flight and arrives in discrete quantities. The second, representing Einstein's hypothesis, is the foundation for photoelectricity and Compton scattering theories, but *a waveform cannot be both travelling and monochromatic* by Lemma 2.1. The hypothesis has stood till now only because the only known transformations of wavelengths had been by Doppler or gravitational shifts or scattering, and not by receiver processing, as in the present case.

In hindsight, the almost instantaneous speed of the photoelectric response and the linear dependence of the peak photoelectron energies on the illuminating frequency had been at odds only with the wave theoretic expectations incorrectly based on the notion of metallic electrons with absorption cross-sections determined by the so-called classical radius of the electron, $r_e \approx 2.82$ fm [2]. Both properties are today well explained in terms of Bloch states characterized by wavelengths that can be in microns, hence with radiation cross-sections 40 orders of magnitude larger! It is safe to interpret Einstein's hypothesis as a temporary correction for those historical expectations, instead of as the final model of the nature of light precluding chirp or any other non-Fourier decompositions.

Spectrometric and Doppler time dilations

In a Fourier diffraction spectrometer, the rays forming an nth order diffraction fringe comprise successive portions of the original wavefronts separated by n wavelengths, i.e., by successive time intervals of $T = n\lambda/c$. Therefore, a drift of grating intervals according to equation (3) equivalently represents a clock drift at the normalized rate $-\beta = (n\lambda)^{-1}\, \partial(n\lambda)/\partial\tau \equiv T^{-1}\, \partial T/\partial\tau$. Using τ to denote time at the receiver, $\langle\tau, -\beta|$ for receiver eigenfunctions in

the presence of such a receiver clock drift, and noting that $\langle\tau,-\beta|\omega'',\beta\rangle \equiv e^{i\omega''\tau}$, we get

$$\langle\tau,-\beta|f,r\rangle \equiv \int_{\omega''}\langle\tau,-\beta|\omega'',\beta\rangle\,d\omega''\,.\,e^{-ik''r}F(\omega''/\Delta) = \int_{\omega''}e^{i\omega''\tau}\,d\omega''\,.\,e^{-ik''r}F(\omega''/\Delta)$$

[substituting $\omega'=\omega''/\Delta$] $\quad = \int_{\omega'}e^{i\omega'\tau\Delta}e^{-i\omega'r\Delta/c}F(\omega')\,d\omega'\Delta \equiv \Delta.f([\tau-r/c]\Delta)\quad,$ (16)

from equation (4). Equation (16) says that *in the presence of a frequency or clock scale drift, a received waveform would appear to be dilated in time, in proportion to its source distance.* Furthermore, *time dilations must hold identically for the mundane Doppler effect*, as we may set the scale drift rate $\beta = 0$ in Δ (equations 10).

The proportionality to source distance makes this effect similar to cosmological time dilation, but even otherwise, this result is remarkable because time dilation as such has been hitherto regarded as an exclusive gift of relativity. All that equation (16) really says is that *a uniform scaling of frequencies means a reciprocal scaling of time.* As the Doppler effect uniform scales the whole spectrum, the *repetition frequencies of pulses* from a moving source should scale by the same amount, so that the pulse intervals would be also dilated, as explained in Fig. 6 below. In retrospect, time dilation has been exotic only because scattering and other matter interactions like the Wolf effect [3], do not uniformly scale the whole frequency axis, as required for the derivation above.
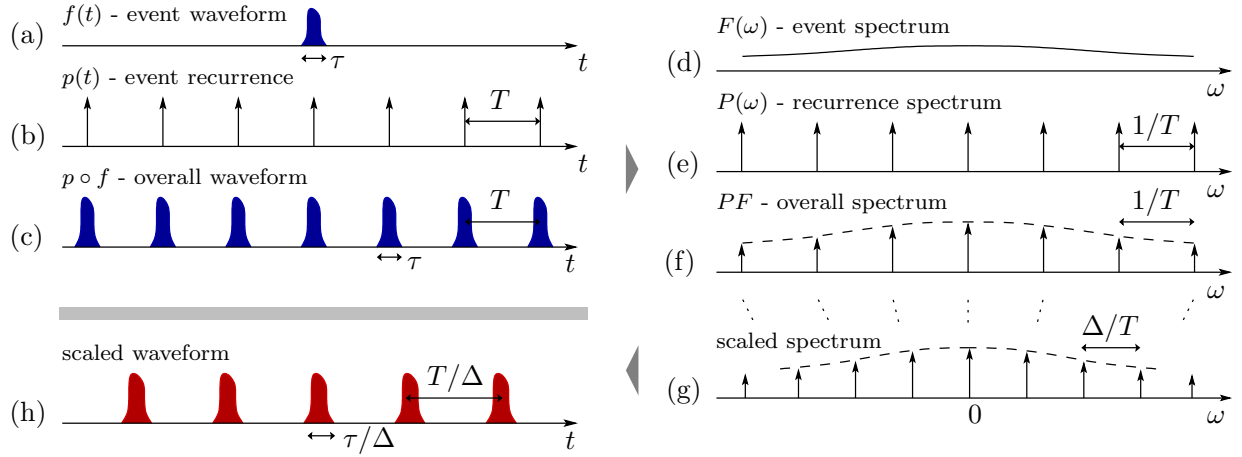
Fig. 6. Analysis of time dilation

Constraint of spectrometric creep on cosmology theory

Whereas the radius of an atom is fundamentally determined by quantum uncertainty (cf. [4, III-§1]), and lattice dimensions are constrained by molecular scale forces, there is no similar guarantee for the macroscopic dimensions of solids. The diffraction gratings or prisms used for frequency or wavelength selection are invariably subject to various thermal and mechanical stresses during operation, and calibration procedures, using onboard as well as distant sources are routinely applied to both ground and orbiting spectrometers used in astronomy. Nevertheless, as the present effect was hitherto unknown, existing calibration procedures were not designed to correct errors due to this effect. Examination of potential causes for triggering this effect and the resulting systematic errors in current data could be a test of the present theory.

In particular, plastic creep is ordinarily small in structural and optical materials that it has not been corrected for even in deep space missions including the Pioneers 10 and 11 and Galileo. However, as treated in the paper, the quantum theory of dislocations in solids predicts a residual creep rate, in the limit of low stresses, of around the same order as the Hubble constant, which has the same dimensions ($[T^{-1}]$). Given the extremely small but nevertheless nonzero compressive stress of gravity due to the curvature of the earth, this residual creep could cause an ongoing shrinkage of both terrestrial and orbiting instruments, including their gratings and prisms, and thus trigger the present effect. Specifically, a shrinkage of grating intervals could cause the diffraction fringes to spread, thereby presenting successively smaller wavelengths, i.e. increasing k', to a fixed detector, and conversely, a shrinkage of the detector array relative to the fringe pattern could present individual detectors with decreasing k'. Thus, the finite rigidity of our spectrometers, which could be represented by an empirical time constant ΔT_E, would allow a scale drift $\Delta\beta$ such that

$$\Delta\beta\,\Delta T_E \approx 1\quad,$$ (17)

posing a systematic uncertainty of up to $\beta = \pm\Delta\beta$ in both distant spectra, according to equation (4), and time scales, by equation (16). Taking $t_\odot \equiv 4.9$ Gy $= 1.55 \times 10^{17}$ s, the age of the sun, as a conservative upper bound, i.e.,

$\Delta T_E \leq t_{\odot}$, yields a scale uncertainty of $\Delta\beta \geq t_{\odot}^{-1} = 200$ km s^{-1} Mpc$^{-1} \approx 2.7 \, H_0$, the Hubble constant. A detailed discussion, revealing consistency with both astrophysical and geological data, is given in the paper.

Undetectability of clock accelerations by local tests

Incidentally, the Pioneer anomaly has been described as equivalent to an apparent onboard clock dilation of the same sign and magnitude as the cosmological time dilation (see [5, 6, 7] and [8, §V-B]). Investigating reference clock stability as a possible source of this anomaly, NASA concluded that the multiple atomic clocks used by the Deep Space Network (DSN) would have had to all have the same drift, which makes it sound unlikely, and noted that their Allan variances, of 10^{-13} to 10^{-15} at the time, precludes any such systematic drift. This questions the preceding implication, even though the sign of the anomaly has been later corrected (cf. [9]).

However, even the latest precision of $\sim 10^{-17}$ s [*Physicsworld.com*, 10 March 2008] remains an order of magnitude larger than the expected creep rate and the anomaly, as both are $\sim H_0 \approx 2.17 \times 10^{-18}$ s^{-1}. Further more, NIST's collection of historical papers [10], in particular [11], reveal that Allan variances are correlations between clocks and auto-correlations of individual clock signals computed by circuit loops. *Any variance by definition measures fluctuations or random variations, and is invalid as a check against a monotonic signal.* The Allan variances are computed by counting down the clock ticks, hence invariant of a systematic speeding up of the clocks. Equations (10) imply that observations of distant sources is necessary for detecting such a systematic local drift.

5. TECHNOLOGICAL SIGNIFICANCE

Scale-free passive ranging

It follows from Fig. 5 that the present effect could be used to determine the distance to an object emitting light or radiation of any kind, without having to measure a round-trip time to the object and back, as in ordinary radar, and also without needing to triangulate from a second receiver location, as commonly used in both astronomy and terrestrial navigation. Even existing passive radars like Lockheed's *Silent Sentry* depend on illumination from terrestrial sources, from which bistatic round-trip times can be effectively calculated for the detection and imaging of flying targets. While the effect would not be useful for detecting and ranging silent hostile targets, it could be immensely useful in rescue, recovery and tracking applications, for example, for quickly locating a beacon transmitter instantly and without triangulation. As a navigational aid, the effect would allow a receiver to instantly and accurately determine the ranges to multiple GPS (or Galileo) satellites *without depending on the encoded time signals*. It could be also used to simplify and improve synthetic aperture imaging, by obviating the very need for processing of round-trip times [12]. Best of all, the instant passive ranging capability provides a single, almost zero-power ranging technology that can be implemented in hand-held devices like cell-phones, depending on the wavelengths and receiving sensitivity of interest, and could be used from mundane automotive collision avoidance to the most distant galaxies and supernovae!

Universal frequency reuse and jamming immunity

Fig. 5 further suggests that we could distinguish between signals of the same carrier frequency ω_c, from two or more sources at different distances r, r', etc. arriving simultaneously at a receiver. This is what would happen if all radio stations within receiving range decided to broadcast at ω_c at the same time, or if someone operated a jammer to block reception at ω_c. The interference and jamming can be eliminated using the present effect by applying a first band-pass filter G_b to limit the received total RF or IF signal to around ω_c; then a time-varying frequency or wavelength selection (or tuning) $H(\beta)$, which would cause simultaneous scaling of the individual signals by different scale factors Δ, Δ', etc., to bands around ω_c/Δ, ω_c/Δ', and so on, respectively, for the same normalized variation rate β; then a second band-pass filter $\widetilde{G}_m$ centred around exactly one of ω_c/Δ, ω_c/Δ', etc., and lastly, a second time-varying tuning mechanism or a down-converter to return the final signal to ω_c [13].

The filtering steps and the final down-conversion are clearly signal processing operations. However, the key step of time-varying frequency or wavelength selection would be able to separate the sources in the frequency domain only because of the present effect representing a fundamental property of wave propagation, which makes it an exact geometrical complement to the angular separation provided by directional antennas (Fig. 7). It is proved in the paper that this would enable physical channels to be simultaneously reused at asymptotically linear distance intervals by indefinitely many sources, *independently of existing modulation and coding technologies*. Moreover, such a receiver would be also able to exclude noise as well as hostile interference and strong jamming within the conventional channel if it is able to discriminate these unwanted sources by direction and range.
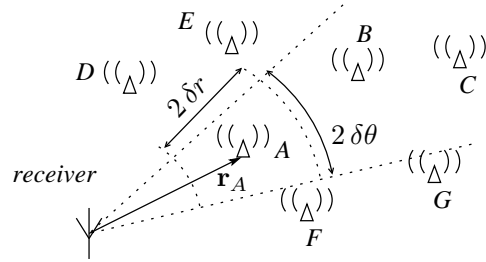
Fig. 7. Signal selection by direction and range

Universal wavelength transformation and synthesis

The effect presents the first general method for transforming wavelengths without motion as in the Doppler effect, or interaction with matter, as in scattering and harmonic generation processes. The transformation capability could have direct utility, for example, for imaging at invisible wavelengths, and in conjunction with available sources to synthesize radiation at other wavelengths, as discussed in the paper.

6. VALIDATION AND PRACTICALITY

This predicted capability of chirp decompositions for scaling spectra in proportion to their source distances has been computationally verified by simulating sources with continuous linespreads as expected for all real sources and applying time-varying, or "chirped" sampling, as explained for Doppler time dilation (equation 16). Fig. 8 is a set of plots obtained from this exercise, for a hypothetical scenario of four 100 THz (1.54 μm) sources located at intervals of 10 km along an optical fibre of refractive index 1.47. As discussed in the paper, multiple methods of simulating the linespreads have been tried and yield the same result. The simulation applet itself is available online at `http://www.inspiredresearch.com`.
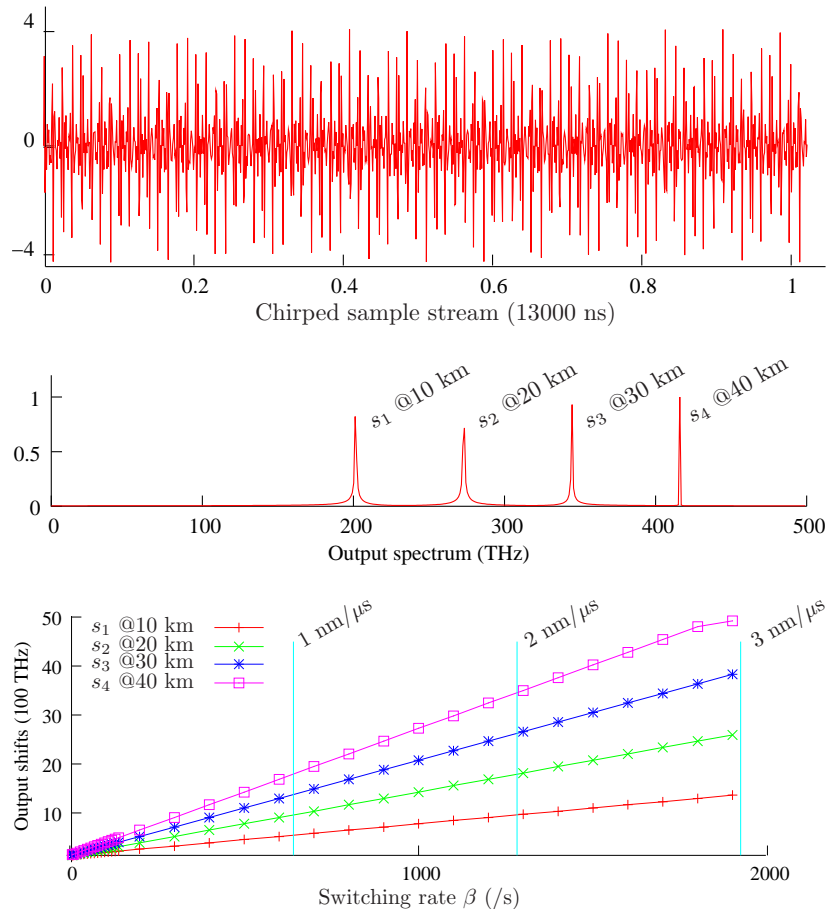

Fig. 8. Verification of the effect by chirped sampling

The applet simulations also explain why the effect had not been discovered serendipitously: the speed of light is so high that mechanisms available for varying frequency or wavelength selection have been relatively too slow to produce observable shifts at laboratory distances of a few metres. Optical switching devices are currently limited to millisecond speeds, whereas even with microsecond speeds, we would need tens of kilometres of optical path. Nanosecond switching devices are being researched, however, and should soon make this effect realizable.

The corresponding difficulty for radio frequency (RF) validation has been in implementing, at the RF front-end, a reliable analogue varactor circuit that can be operated independently of the carrier selection, and equivalently, over-sampling at (GHz) frequencies that can be reliably tested within an anechoic chamber for robust validation. The solution seems to be to test at intermediate frequencies (IF), as the trigonometric identities

$$
\begin{aligned}
\cos(\psi_c) \times \cos(\psi_o) &= \cos(\psi_c + \psi_o) + \cos(\psi_c - \psi_o) \\
-\sin(\psi_c) \times \sin(\psi_o) &= \cos(\psi_c + \psi_o) - \cos(\psi_c - \psi_o) \ ,
\end{aligned}
\tag{18}
$$

holds not just for carrier and local oscillator (LO) frequencies as $\psi_c \sim \omega_c t$ and $\psi_o \sim \omega_o t$, as generally expressed in engineering literature, but actually for the full instantaneous phases $\psi_c \equiv \omega_c t + \phi_c$ and $\psi_o \equiv \omega_o t + \phi_0$, where ϕ_c and ϕ_o denote the respective phase offsets, implying that *four-quadrant mixing preserves RF phase*. The effect should be therefore readily realizable in existing radios and cell-phones.

Lastly, the present effect seems entirely consistent with astronomical and geological data, including cosmological time dilations and the Tolman brightness test; would account for instrument creep for the first time; and would be consistent with the still missing treatment of cumulative diffraction in astrophysics. It is thus predicated by astronomy for want of immediate terrestrial validation, just as it was for the Doppler effect [14], and if validated by RF or optical tests, would lead to a more conservative theory that does not presume identical Hubble redshifts from extra-terrestrial platforms like mainstream cosmology, as briefly discussed in the paper.

References

[1] M Born and E Wolf. *Principles of optics: electromagnetic theory of propagation, interference and diffraction of light.* Cambridge University Press, seventh (expanded) edition, 2002.

[2] R A Millikan. A Direct Photoelectric Determination of Planck's "h". *Phys Rev*, 7:355–388, 1916.

[3] E Wolf. Non-cosmological redshifts of spectral lines. *Nature*, 326:363–365, 1987.

[4] R P Feynman, R Leighton, and M Sands. *The Feynman Lectures on Physics.* Addison-Wesley, 1964.

[5] J D Anderson et al. Indication from Pioneer 10/11, Galileo and Ulysses data of an apparent anomalous, weak, long-range acceleration. *Phys Rev Lett*, 81:2858–2861, Oct 1998. Also: gr-qc/9808081.

[6] J L Rosales and J L Sanchez-Gomez. A possible cosmological origin of the indicated anomalous acceleration ... *gr-qc/9810085*, Oct 1998.

[7] R Ellman. An interpretation of the Pioneer 10/11 ... *Phys Rev Lett*, 81(14):5, Oct 1998.

[8] J D Anderson et al. Study of the anomalous acceleration of Pioneer 10 and 11. *Phys Rev D*, 65:082004/1–50, Apr 2002. Also: report LA-UR-00-5654 and gr-qc/0104064.

[9] V T Toth and S G Turyshev. The Pioneer Anomaly: seeking an explanation in newly recovered data. *gr-qc/0603016*, Mar 2006.

[10] (eds.) D B Sullivan, D W Allan, D A Howe, and F L Walls. Characterization of Clocks and Oscillators. Technical report, NIST, Mar 1990. Report No. 1337.

[11] D A Howe, D W Allan, and J A Barnes. Properties of signal sources and measurement methods. *Proc IEEE 35th Ann. Symp. Freq. Control*, 1981. (reprinted in NIST Technical Note 1337, 1990).

[12] V Guruprasad. A wave effect enabling universal frequency scaling, monostatic passive radar, incoherent aperture synthesis, and general immunity to jamming and interference. In *MILCOM'2005 (classified session)*, Oct 2005.

[13] V Guruprasad. Relaxed bandwidth sharing with Space Division Multiplexing. In *IEEE Wireless Comm. and Networking Conference*, March 2005.

[14] J C A Doppler. *On the coloured light of the binary stars and other celestial bodies.* Prague: K Bohm Gesellschaft der Wissenschaften, 1842. (in German).